Atmos. Chem. Phys., 12, 4327–4340, 2012
www.atmos-chem-phys.net/12/4327/2012/
doi:10.5194/acp-12-4327-2012

Atmospheric Chemistry and Physics

Estimation of speciated and total mercury dry deposition at monitoring locations in eastern and central North America

L. Zhang[1], P. Blanchard[1], D. A. Gay[2], E. M. Prestbo[3], M. R.Risch[4], D. Johnson[5]

precipitation (Vanarsdale et al., 2005; Prestbo and Gay, 2009; Risch et al., 2012b). More recently, the Atmospheric Mercury Network (AMNet) of NADP was also established to

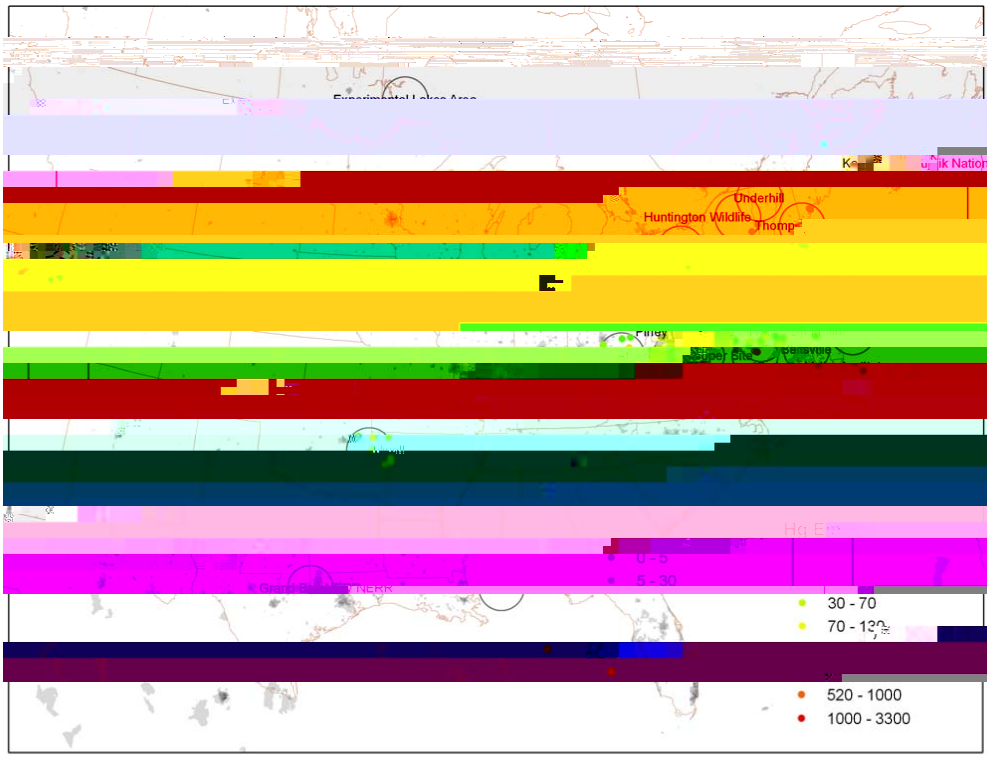

Fig. 1. Locations of the AMNet sites where Hg dry deposition were estimated. Also shown are Hg point source emissions with a 100 km

Table 1. List of AMNet site information.

AMNet Site ID	Site Name	Lat and lon	Data coverage	Dominant land type within 1 km circle	Site category
MD08	Piney Reservoir	39.7053, −79.0122	Jan 2008–Dec 2009	Grass, mixed forest, shrubs, lake	rural
MD99	Beltsville	39.0284, −76.8171	Jan–Feb 2008, May–Jun 2008, Apr–Sep 2009, Dec 2009	Forest, urban	suburban
MS12	Grand Bay NERR	30.4294, −88.4277	Jan 2008–Dec 2009 except Sep 2008	Woody wetland, shrubs, forest,	rural
NH06	Thompson Farm	43.1100, −70.9500	Feb 2009–Dec 2009	Mixed forest, crops	rural

underestimated where PBM are frequently associated with coarse particles.

The original model of Zhang et al. (2001) used 15 LUCs, but here we used 26 LUCs (Table S1), following Zhang et al. (2003). Input parameters in Zhang et al. (2001) were given for each LUC and for five seasonal categories. This approach was discarded here; instead, the same approach developed in Zhang et al. (2003) was used. That is, for any input parameter (X) changing with season, a maximum value ($X_{\max}$) and a minimum value ($X_{\min}$) were provided and were then interpolated to any day of the year based on the annual variation of the leaf area index (LAI):

$$X(t) = X(\min) + \frac{\mathrm{LAI}(t) - \mathrm{LAI}(\min)}{\mathrm{LAI}(\max) - \mathrm{LAI}(\min)}[X(\max) - X(\min)]$$

where t represents any day of the year, and LAI(min) and LAI(max) represent minimum and maximum LAI values, respectively, during the year. Input parameters for the particle dry deposition model that need interpolation include a parameter for the characteristic radius of collectors, a parameter for calculating the collection efficiency by Brownian diffusion, and a parameter for calculating the collection efficiency by impaction (Zhang et al., 2001). Roughness for each LUC for the particle dry deposition model is the same as for the gaseous dry deposition model, as described in Zhang et al. (2003).

The meteorological data used for driving the dry deposition models were from the archived data produced by the Global Environmental Multiscale model, which is the Canadian weather forecast model, an approach described in Brook et al. (1999). Meteorological variables representing the same time period as the Hg air concentration measurements for the surface and the first model-layer, typically at 40–50 m in height, are available hourly at a horizontal grid resolution of 15 km by 15 km. Data for model grids containing the measurement sites were extracted from the archived data to calculate hourly V_d. Area-weighted land types within a 1 km radius of each site were used to calculate V_d (see Table 1 and Table S1).

2.4 Litterfall and wet deposition measurements

To assess the reasonableness of these dry deposition estimates, and explore the sources of Hg in litterfall, estimated speciated and total Hg dry deposition were compared with collected litterfall Hg. The total net Hg dry deposition to a forest is the sum of the Hg in the litterfall, the Hg captured by the canopy and then emitted back to the atmosphere, the Hg washed off the canopy by precipitation (throughfall), and the Hg deposited directly to the underlying soils. Thus, litterfall deposition may be treated as the low-end estimation of the total Hg dry deposition to a forest, if Hg emission from the underlying soil is limited. On the other hand, if soil Hg emissions are high and the ambient Hg concentrations above the forest are low, the litterfall Hg might be higher than the dry deposition above the canopy due to the interception of emitted Hg by the forest leaves. Based on the above arguments, it is reasonable to assume that total dry deposition and litterfall deposition should be similar on regional scales, although the differences can be very large at individual sites. Thus, we compared the estimated dry deposition with measured litterfall deposition on a regional-scale and at six collocated sites (see below for details). A better comparison would be to compare the estimated dry deposition with the litterfall plus throughfall deposition, as was also done for ELA in this study.

Three-year average Hg litterfall measurements during 2007–2009 at 23 selected MDN sites, as described in detail by Risch et al. (2012a), were used for this study. The site information for the litterfall measurements is listed in Table S2. Litterfall measurements were also made at the ELA site (Graydon et al., 2008). Note that many AMNet sites are not collocated with MDN sites and thus are not at the same sites where the litterfall data were collected. Only six sites have both dry deposition estimation and litterfall measurements (Table 2).

Wet deposition collected by MDN during the years 2007-2009 were also used for the purpose of quantifying the relative importance of dry and wet deposition. A wet deposition map was created using the three-year average wet deposition of non-urban MDN monitoring sites. For this data, non-urban sites were defined as less than 400 people per square kilometer (km^2) within a 15 km radius of the site. The interpolated annual sums of Hg wet deposition were computed for an array of regularly spaced grid values using the sites that were within 300 km of each grid point. The boundary of the interpolated area was trimmed at the coast line and smoothed for values up to 300 km from the outermost data points over land.

3 Results and discussion

3.1 Air concentrations

Annual average concentrations among the sites during 2008–2009 ranged from 1.1 to 22.6 $\mathrm{pg\,m^{-3}}$ for GOM, 2.9 to 17.1 $\mathrm{pg\,m^{-3}}$ for PBM, and 1.2 to 2.1 $\mathrm{ng\,m^{-3}}$ for GEM (Fig. 2a, b). As expected, the species having the shortest lifetimes had the largest geographical variations. GOM only contributed 0.1–1.5 % to the total gaseous Hg (GOM+GEM) at these locations.

The highest annual concentrations for GEM were detected at several urban and suburban sites (e.g., 1.79 to 2.13 $\mathrm{ng\,m^{-3}}$ for NJ32, NJ54, NJ30, and UT97), whereas the lowest annual concentrations were detected in more remote rural areas (e.g., 1.24 to 1.37 $\mathrm{ng\,m^{-3}}$ for ELA, NH06, OK99, and NS01). The annual GEM concentrations did not differ significantly between suburban and rural sites in the north-eastern

Table 2. Estimated speciated and total dry deposition ($\mu g\,m^{-2}\,yr^{-1}$) and measured litterfall deposition ($\mu g\,m^{-2}\,yr^{-1}$) at six sites. The last column represents upper-end estimation of GOM+PBM dry deposition by incorporating the potential uncertainties.

Site ID	GOM	PBM	GOM+PBM	Net GEM	Total dry deposition	Litterfall	Increased GOM+PBM
MD08	7.8	0.30	8.1	6.8	14.9	15.3	16.8
MD99	1.3	0.32	1.6	9.0	10.6	15.5	3.9
OH02	3.0	0.38	3.4	9.9	13.3	18.8	7.5
VT99	0.72	0.41	1.1	11.7	12.8	11.3	3.1
WV99	3.6	0.44	4.0	8.2	12.2	9.9	9.0
ELA	0.49	0.25	0.74	15.6	16.3	8.6	2.0

USA due to the many point and area sources in this region (Fig. 1) and the long atmospheric lifetime of GEM. The geographical variations in the annual GEM were within a factor of 1.8 among all of the sites discussed here. As with GEM, the lowest annual concentrations of GOM and PBM were also detected at the same remote rural sites (ELA, NH06, OK99, and NS01); however, this was not the case for the highest concentrations of GOM and PBM. For example, UT97, MD08, WV99, and OH02 had the highest GOM concentrations and UT96, UT97, and NJ54 had the highest PBM concentrations. Similar to GEM, quite a few rural sites (e.g., WV99, OH02, and MD08) had GOM and PBM concentrations that were comparable to the concentrations at the urban and suburban sites. Among all of the sites, the geographical variations in the annual GOM were within a factor of 20,

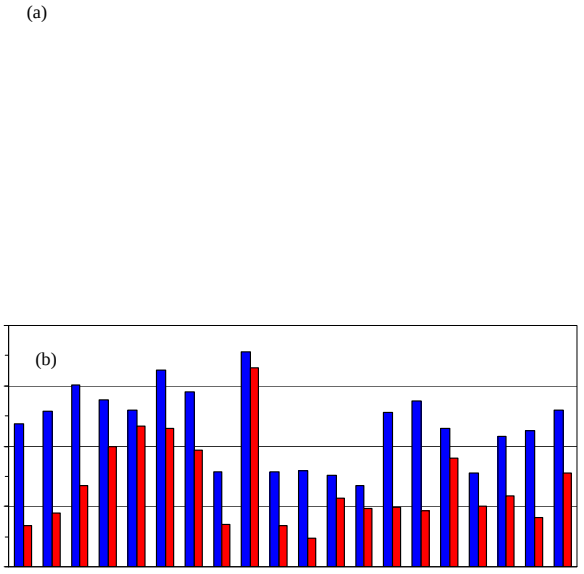

Fig. 3. Annual average speciated dry deposition fluxes ($\mu g\,m^{-2}$). Net GEM flux is the GEM dry flux minus GRAHM modeled annual GEM re-emission and natural emission fluxes.

3.2 deposition velocities

Based on existing models/parameterizations constructed for the calculation of Hg V_d (e.g., Zhang et al., 2009 and references therein), if meteorological conditions are similar, GOM and PBM should have larger V_d values over surfaces with larger roughness lengths (and thus higher friction velocities) than over smoother surfaces; and GEM should have larger V_d values over canopies with larger LAI than over any other surface. For example, the estimated annual V_d of GOM over forest-dominated sites was in the range of 1.4–2.0 $cm\,s^{-1}$, and was close to 1.0 $cm\,s^{-1}$ over urban areas (Fig. 2c). Values lower than 0.8 $cm\,s^{-1}$ were also calculated for a few sites with small roughness lengths and/or weak wind speeds. In general, estimated V_d of PBM was five to ten times smaller than V_d of GOM. Estimated annual V_d for GEM was mostly in the range of 0.05–0.08 $cm\,s^{-1}$ over vegetated surfaces and below 0.05 $cm\,s^{-1}$ over urban areas, and was generally 20–30 times smaller than those of GOM, and 2–6 times smaller than PBM. Calculated V_d values shown here are well within the range of published estimates (Zhang et al., 2009).

The estimated seasonal (or monthly) average V_d for GOM and PBM was higher during seasons with strong wind speeds. Note that R_a, R_b, R_{ns} and R_s, defined in Sect. 2.4, are all smaller under stronger wind conditions. As for GEM, the V_d was higher over forests and during full growing seasons than over other surfaces or during other seasons due to the dominant effect of LAI on V_d. As an example, average diurnal and monthly V_d at the Kejimkujik site (NS01; a remote coastal site with forest coverage) are shown in Fig. S2 in the Supplement. The wind was stronger in the winter than in the summer at this location and thus V_d values of GOM and PBM were higher in the winter. On the other hand, V_d of GEM was much higher in the spring and summer than in the winter due to the dominant effect of LAI. The relative changes (compared to their own annual average values) in the seasonal and diurnal V_d were also much larger for GEM (see normalized V_d, Fig. S2 in the Supplement).

3.3 Estimated dry deposition fluxes

The estimated annual dry deposition of GOM+PBM ranged from 0.4 to 8.1 $\mu g\,m^{-2}\,yr^{-1}$ at the 19 sites. GOM contributed 0.3-7.8 $\mu g\,m^{-2}\,yr^{-1}$ to these fluxes, whereas PBM contributed only 0.1–0.8 $\mu g\,m^{-2}\,yr^{-1}$ (Fig. 3a). The estimated annual GEM dry deposition was in the range of 13 to 35 $\mu g\,m^{-2}\,yr^{-1}$ (Fig. 3b), much higher than originally assumed in many previous studies. Earlier studies either simply excluded GEM in the dry deposition budget or used extremely small V_d values (Engle et al., 2010; Baker and Bash, 2012). Despite the high V_d values used for GEM in the present study, dry deposition estimates for GEM are still believed to be conservative estimates, as mentioned in Sect 2.3. The very high dry deposition fluxes of GEM are certainly due to the two to three orders of magnitude higher concentrations of GEM compared to those of GOM+PBM. As discussed in Zhang et al. (2012a), GEM re-emission was around half of the GEM dry deposition on regional scales in eastern North America, although the relative importance of re-emission/dry deposition varied significantly with locations. Using GRAHM modeled GEM re-emission and natural emission, net GEM dry deposition fluxes were estimated to be in the range of 4.8 to 23.3 $\mu g\,m^{-2}\,yr^{-1}$ for all of the sites except for NS01, at 33 $\mu g\,m^{-2}\,yr^{-1}$ (Fig. 3b). The estimated net GEM dry deposition was still much higher than the estimated GOM+PBM dry deposition at the majority of the monitoring sites. It is noted that at several sites (MD08, UT07, WV99), net GEM dry deposition and dry deposition of GOM+PBM were in a similar range of values (within a factor of 2).

Estimated dry deposition of GOM+PBM was mostly two to five times higher at sites near significant Hg emissions (e.g., point sources $>200\,kg\,yr^{-1}$) than at the remote sites, but this is not the case for the estimated net GEM dry deposition. This is due to the strong dependence of GEM V_d on land types, meteorological conditions, and the small geographical variations of the ambient GEM concentrations. For example, the dry deposition of GOM+PBM was among the lowest at several rural/remote sites (ELA, Kejimkujik, Underhill), while the net GEM dry deposition at these locations was among the highest. Thus, the total dry deposition does not necessarily correlate with proximity to emission sources due to the dominance of GEM dry deposition.

These estimated annual GOM dry deposition amounts were in the same range as those in several previous studies based on measured ambient GOM concentrations. For example, Engle et al. (2010) and Lombard et al. (2011) obtained GOM dry depositions in the range of 0.5 to 5.3 $\mu g\,m^{-2}\,yr^{-1}$ at multiple locations in central and eastern USA; the only exception was for an urban site (Illinois) with estimated GOM deposition of 52 $\mu g\,m^{-2}\,yr^{-1}$, due to extremely high GOM concentrations. Here, estimated GOM dry deposition ranged from 0.3 to 4.5 $\mu g\,m^{-2}\,yr^{-1}$ for all of the sites except for MD08, which was 7.8 $\mu g\,m^{-2}\,yr^{-1}$.

The estimated GOM+PBM dry deposition in the present study seems to be supported by limited field measurements using surrogate surfaces at several sites (MD08, NY20, and NY95). For example, Castro et al. (2012) obtained an annual dry deposition of 3.2 $\mu g\,m^{-2}\,yr^{-1}$ for GOM at MD08. However, the average GOM concentration during their study period (September 2009 to October 2010) was 9.1 $pg\,m^{-3}$. In comparison, the annual average GOM concentration from the present study was 21.5 $pg\,m^{-3}$ and the estimated dry deposition was 7.8 $\mu g\,m^{-2}\,yr^{-1}$ (Figs. 2, 3). Model estimations agree reasonably well with surrogate-surface measurements at this site after concentration adjustments (e.g., $<10\,\%$ difference). Measured GOM+PBM dry deposition at NY20 during April 2009 to January 2010 was 0.8 $\mu g\,m^{-2}\,yr^{-1}$ and at NY95 during January to November 2009 was 4.4 $\mu g\,m^{-2}\,yr^{-1}$ (Huang et al., 2012). In comparison, the estimated dry deposition was 0.4 $\mu g\,m^{-2}\,yr^{-1}$ at NY20 during 2008 and was 3.9 $\mu g\,m^{-2}\,yr^{-1}$ at NY95 for September 2008 to December 2009. At NY20, the average GOM concentration was 1.9 $\mu g\,m$

good agreement (e.g., within 30 % difference) between the model estimates and the surrogate-surface measurements at several sites discussed in Sect. 3.3 support this. However, an earlier study by Lyman et al. (2007), using a modified version of the present model, found the model underestimated GOM dry deposition by a factor of 2 or more compared with their surrogate-surface measurements. They also stated that the model results were sensitive to environmental and meteorological conditions, and application of the model to other land use categories or climatological conditions would likely yield different results. Huang et al. (2012), on the other hand, found much closer agreements between the model estimates and the surrogate-surface measurements, with the model estimates lower by 10 % to 50 % (or a factor of 2), depending on the location and the sampling method, rather than on the measurements. The same study also found the dry deposition measured using different surrogate surfaces differed by nearly a factor of 1.8. Thus, it is believed that uncertain-

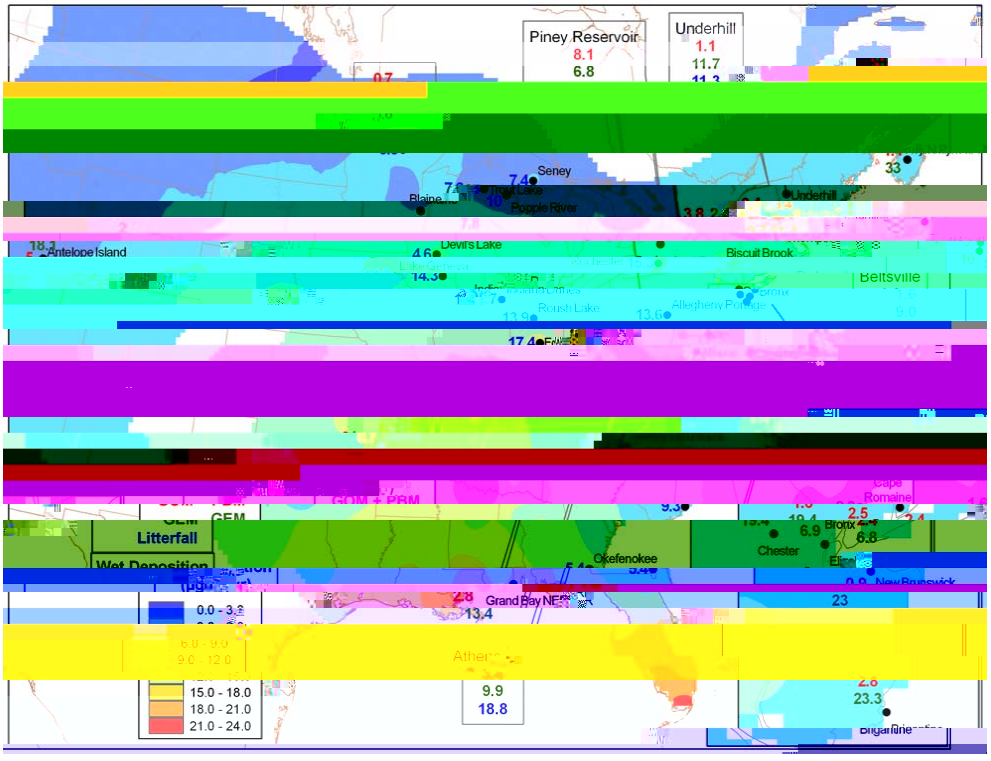

Fig. 4. Comparisons of estimated dry deposition of GOM+PBM and GEM from 2008 and 2009 speciated concentrations with litterfall deposition collected during 2007–2009 and with wet deposition monitored during 2007–2009.

GEM dry deposition explains 45–60 % of the litterfall deposition while the total dry deposition explains □70–100 % of the litterfall deposition. There are several possibilities causing these discrepancies: (1) dry deposition of GOM+PBM and the net GEM were underestimated due to various reasons, including the overestimation of GEM re-emission; (2) if only using forest canopies for estimating dry deposition at these three sites (nearly 50 % of the areas were not forests at these three sites as shown in Table S1), the net GEM dry de-

Table 3. Estimated annual dry deposition ($\mu g\,m^{-2}\,yr^{-1}$) and measured annual wet deposition ($\mu g\,m^{-2}\,yr^{-1}$) at AMNeT/MDN collocated sites. Three-year average annual precipitation amount (cm) is also shown.

AMNet/MDN Site ID	Site Name	Site Category	GOM+PBM	Net GEM	Total dry	Wet	Dry/wet	Precip
MD08	Piney Reservoir	Rural	8.1	6.8	14.9	8.3	1.8	110
MD99	Beltsville	Suburban	1.6	9.0	10.6	9.7	1.1	112
NJ30	New Brunswick	Urban	0.9	23	23.9	8.6	2.8	126
NS01	Kejimkujik National Park	Rural	1.4	33	34.4	7.1	4.8	147

et al. (2005). But the relative contribution of dry and wet deposition to the total deposition certainly depends on location, season, and meteorological conditions.

4 Conclusions and recommendations

Despite the potentially large uncertainties in the concentration measurements and in the calculated deposition velocities, the estimated dry deposition of GOM+PBM agrees with the limited surrogate-surface dry deposition measurements and the estimated annual total dry deposition (GOM+PBM+net GEM) is in the same range as the annual litterfall Hg measurements. This provides some confidence on the estimated dry deposition. The results presented here suggest that GEM contributes much more than GOM+PBM to the total dry deposition at the majority of the sites studied here; the only exception is at the locations close to significant point sources where GEM and GOM+PBM contribute equally to the total dry deposition. This also implies that litterfall Hg is largely from the collection of GEM. Dry deposition has a similar value range to wet deposition, and thus needs to be quantified as accurately as possible.

Future work should focus on estimating net GEM dry deposition more accurately, especially considering its dominant role as a contributor to the total dry deposition. This will involve a better handling of the bi-directional exchange process, and a better understanding of GEM emission from natural surfaces. Recently, several research groups in the United States started measuring GEM gradients over forest canopies (10th ICMGP, Halifax, Canada, 23–29 July 2011). These measurements, together with modeling practices, should improve our understanding of net GEM dry deposition. It is recommended, wherever possible, to collect data that can be used to quantify GEM fluxes, both above the canopy and above the forest floor, so that the data can be used to develop and improve bi-directional exchange models for GEM.

Supplementary material related to this article is available online at: http://www.atmos-chem-phys.net/12/4327/2012/acp-12-4327-2012-supplement.pdf.

Acknowledgements. L. Zhang greatly appreciates I. Cheng for helpful discussion, A. Dastoor and A. Ryzhkov for providing GRAHM modeled GEM emission data, and AMNet site operators for their contribution in the collection of the speciated mercury ambient concentration data.

Edited by: J . H. Seinfeld

References

Amos, H. M., Jacob, D. J., Holmes, C. D., Fisher, J. A., Wang, Q., Yantosca, R. M., Corbitt, E. S., Galarneau, E., Rutter, A. P., Gustin, M. S., Steffen, A., Schauer, J. J., Graydon, J. A., Louis, V. L. St., Talbot, R. W., Edgerton, E. S., Zhang, Y., and Sunderland, E. M.: Gas-particle partitioning of atmospheric Hg(II) and its effect on global mercury deposition, Atmos. Chem. Phys., 12, 591–603, doi:10.5194/acp-12-591-2012, 2012.

Atmospheres, 115, D18306, doi:10.1029/2010JD014064, 2010.
Evers, D. C., Jackson, A. K., Tear, T. H., and Osborne, C. E.: Hidden Risk: Mercury in Terrestrial Ecosystems of the Northeast, Biodiversity Research Institute, Gorham, Maine, 33 pp., 2012.
Flechard, C. R., Nemitz, E., Smith, R. I., Fowler, D., Vermeulen, A. T., Bleeker, A., Erisman, J. W., Simpson, D., Zhang, L., Tang, Y. S., and Sutton, M. A.: Dry deposition of reactive nitrogen to European ecosystems: a comparison of inferential models across the NitroEurope network, Atmos. Chem. Phys., 11, 2703–2728, doi:10.5194/acp-11-2703-2011, 2011.
Friedli, H. R., Arellano, A. F., Cinnirella, S., and Pirrone, N.: Initial estimates of mercury emissions to the atmosphere from global biomass burning, Environ. Sci. Technol., 43, 3507–3513, 2009.
Gbor, P. K., Wen, D., Meng, F., Yang, F., and Sloan, J. J.: Modeling of mercury emission, transport and deposition in North America, Atmos. Environ., 41, 1135–1149, 2007.
Graydon, J. A., St. Louis, V. L., Hintelmann, H., Lindberg, S. E., Sandilands, K. A., Rudd, J. W. M., Kelly, C. A., Hall, B. D., and Mowat, L. D.: Long-term wet and dry deposition of total and methyl mercury in the remote boreal ecoregion of Canada, Environ. Sci. Technol., 42, 8345–8351, 2008.
Graydon, J. A., St. Louis, V. L., Hintelmann, H., Lindberg, S. E., Sandilands, K. A., Rudd, J. W. M., Kelly, C. A., Tate, M. T., Krabbenhoft, D. P., Lehnherr, I.: Investigation of uptake and retention of atmospheric Hg(II) by boreal forest plants using stable Hg isotopes, Environ. Sci. Technol., 43, 4960–4966, 2009.
Gustin, M. S. and Jaffe, D.: Reducing the Uncertainty in Measurement and Understanding of Mercury in the Atmosphere, Environ. Sci. Technol., 44, 2222–2227, 2010.
Gustin, M. S., Lindberg, S. E., and Weisberg, P. J.: An update on the natural sources and sinks of atmospheric mercury, Appl. Geochem., 23, 482–493, 2008.
Huang, J., Choi, H.-D., Hopke, P. K., and Holsen, T. M.: Ambient Mercury Sources in Rochester, NY: Results from Principle Com-